ARMY RESEARCH LABORATORY

Another Analytical Approach to Predicting Munition Trajectories

by Gene R. Cooper, Paul Weinacht, and James F. Newill

ARL-TR-3948 **September 2006**

NOTICES

Disclaimers

The findings in this report are not to be construed as an official Department of the Army position unless so designated by other authorized documents.

Citation of manufacturer's or trade names does not constitute an official endorsement or approval of the use thereof.

Destroy this report when it is no longer needed. Do not return it to the originator.

Army Research Laboratory
Aberdeen Proving Ground, MD 21005-5066

ARL-TR-3948 **September 2006**

Another Analytical Approach to Predicting Munition Trajectories

Gene R. Cooper, Paul Weinacht, and James F. Newill
Weapons and Materials Research Directorate, ARL

REPORT DOCUMENTATION PAGE

Form Approved
OMB No. 0704-0188

1. REPORT DATE *(DD-MM-YYYY)*	2. REPORT TYPE	3. DATES COVERED (From - To)
September 2006	Final	20 October 2005–31 July 2006

4. TITLE AND SUBTITLE
Another Analytical Approach to Predicting Munition Trajectories

5a. CONTRACT NUMBER

5b. GRANT NUMBER

5c. PROGRAM ELEMENT NUMBER

6. AUTHOR(S)
Gene R. Cooper, Paul Weinacht, and James F. Newill

5d. PROJECT NUMBER
688618.H80

5e. TASK NUMBER

5f. WORK UNIT NUMBER

7. PERFORMING ORGANIZATION NAME(S) AND ADDRESS(ES)
U.S. Army Research Laboratory
ATTN: AMSRD-ARL-WM-BC
Aberdeen Proving Ground, MD 21005-5066

8. PERFORMING ORGANIZATION REPORT NUMBER
ARL-TR-3948

9. SPONSORING/MONITORING AGENCY NAME(S) AND ADDRESS(ES)

10. SPONSOR/MONITOR'S ACRONYM(S)

11. SPONSOR/MONITOR'S REPORT NUMBER(S)

12. DISTRIBUTION/AVAILABILITY STATEMENT
Approved for public release; distribution is unlimited.

13. SUPPLEMENTARY NOTES

14. ABSTRACT
Analysis presented here addresses a previous problem concerning free-flight projectiles governed by the two-dimensional, point mass equations representing drag as a power law. Down-range distance is taken to be the independent variable which yields a third-order differential equation governing the projectile's flight. An approximate solution is obtained which is shown to be very accurate for gun elevation angles up to 30°. Previously examined engineering characteristics for flat fire are reconsidered here with nonzero elevation angles over a range of projectile flight parameters. An important change from previous work is that gravity is never neglected when using the various parameterized drag curves, thus the velocity drag relation has gravity dependence. Firing table drag data are employed to study several examples using this analysis. Comparisons between analytical and numerical models to previous work are presented. This report shows that the results given here offer another simple means to examine the performance of low-yaw/high-velocity projectiles where the launch angle is as high as 30°.

15. SUBJECT TERMS
trajectory, 2-D equations, power law drag

16. SECURITY CLASSIFICATION OF:			17. LIMITATION OF ABSTRACT	18. NUMBER OF PAGES	19a. NAME OF RESPONSIBLE PERSON
a. REPORT	b. ABSTRACT	c. THIS PAGE			Gene R. Cooper
UNCLASSIFIED	UNCLASSIFIED	UNCLASSIFIED	UL	26	19b. TELEPHONE NUMBER (*Include area code*) 410-278-3684

Contents

List of Figures

List of Tables

1. Introduction

Analysis and predictions of projectile trajectories has a long history. Notable authors are Galileo, Bernoulli, and Euler who found mathematical solutions to this problem which gave important advances to trajectory predictions. Newton has been credited for the quadratic law of resistance characterizing the aerodynamic drag of a body. Further study has shown that a more sophisticated characterization of drag is required to predict accurate trajectories. Weinacht et al. (*1*) give a nice historical perspective of previous work followed by a detailed analysis of trajectories based on power-law drag curves. Increased sophistication has also lead to some unfortunate consequences. Details are often required that may not always be relevant to the problem in question and thus over-burdening the user or designer. For such cases, simplified analysis can provide accurate results with a minimum of relevant input.

High-velocity, direct-fire munitions can be studied using point mass trajectory equations coupled a with power-law drag relation (*1–4*). The study (*1*), suggested by the experimental study of Celmins (*5*), presented analysis and predictions of flat-fire projectiles with small yaw and high velocities using a drag law of the form:

$$C_D = C_D\big|_{V_0} \left(\frac{V_0}{V} \right)^n \quad . \tag{1}$$

The governing equations assumed two-dimensional (2-D) motions with parameterized drag curves depicting drag for projectile velocities that result in high Mach numbers. The analysis was done by first neglecting gravity and finding closed-form solutions to the zero gravity velocity profiles. Then motion under the influence of gravity was modeled using drag forces (equation 1) subjected to these zero gravity velocities.

A continuation of this work is given here but this analysis retains gravity such that drag is always influenced by gravity while using the same power-law drag formulation found in Weinacht et al. (*1*). The vertical and horizontal momentum equations are shown to be equivalent to a single third-order differential equation (DE) in which the independent variable is the down-range distance. Making the assumption that the explicit slope of the trajectory DE can be written as a free parameter allows the governing third-order DE to be integrated giving simple closed-form solutions. When the launch angle is small, these solutions become the solutions found in Weinacht et al. (*1*). A value for the free parameter is given and is shown to produce very accurate closed-form solutions for launch angles up to 30°. These solutions yield easy-to-use results that broaden those given in Weinacht et al. (*1*) for flat-fire cases. The theory and model discussions are presented in the following sections.

2. Equations of Motion

Assuming the 2-D theory found in Weinacht et al. (*1*) gives the governing equation:

$$\dot{\bullet} \equiv \frac{d}{dt}$$

$$\ddot{x} = -\lambda V \left(\frac{V_0}{V}\right)^n \dot{x}$$

$$\ddot{y} = -\lambda V \left(\frac{V_0}{V}\right)^n \dot{y} - g$$

$$V^2 = \dot{x}^2 + \dot{y}^2$$

$$\lambda = \frac{\rho S C_D\big|_{V_0}}{2m}. \qquad (2)$$

Using x as the independent variable leads to $\dot{y} = y'\dot{x}$ and $\ddot{y} = y''\dot{x}^2 + y'\ddot{x}$, so equation 2 becomes:

$$' \equiv \frac{d}{dx}$$

$$y'' = -\frac{g}{\dot{x}^2} \Rightarrow$$

$$y''' = \frac{2g\ddot{x}}{\dot{x}^4} = -\frac{2\lambda g V\left[\frac{V_0}{V}\right]^n}{\dot{x}^3}. \qquad (3)$$

Noting that $V = \dot{x}\sqrt{1+y'^2} = \sqrt{\frac{-g\left(y'^2+1\right)}{y''}}$ gives the following expressions and initial conditions:

$$y''' = -\frac{2V_0^{n-1}V'\big|_0\left[-y''\right]^{\frac{n+2}{2}}}{g^{\frac{n}{2}}\left[y'^2+1\right]^{\frac{n-1}{2}}} \quad y\big|_0 = 0,\ y'\big|_0 = \tan(\phi),\ y''\big|_0 = -\frac{g}{V_0\cos^2(\phi)}. \qquad (4)$$

$$\dot{x} = \sqrt{\frac{-g}{y''}},\ \dot{y} = \dot{x}y',\ x\big|_0 = 0 \text{ and } V'\big|_0 = V_0\lambda.$$

For convenience, two length scales are defined as $y = Y g/V'\big|_0^2$ and $x = X V_0/V'\big|_0$ making the last equation in equation 3 take the form

$$Y''' = -\frac{2\left(-Y''\right)^{\frac{n+2}{2}}}{\left(\left[\frac{g\,Y'}{V_0\,V'|_0}\right]^2+1\right)^{\frac{n-1}{2}}},\ Y|_0 = 0,\ Y'|_0 = \frac{V_0\,V'|_0\tan\phi}{g},\ Y''|_0 = -\frac{1}{V_0\cos\phi}. \tag{5}$$

Please note that equation 5 is equivalent to equation 1 even when $\lambda = \lambda(y)$, but the presentation given here takes $\lambda = \text{constant}$.

The analysis given in Weinacht et al. (*1*) focused on direct fire, thus assuming the elevation angle ϕ is small. This suggests a very good approximation is to let $\left[\frac{g\,Y'}{V_0\,V'|_0}\right]^2 << 1$, which leads to results nearly identical to those given in Weinacht et al. (*1*) if ϕ is small. However, in the interest of using elevation angles ϕ that are not necessarily small, it further suggests treating $Q = \left(\left[\frac{g\,Y'}{V_0\,V'|_0}\right]^2+1\right)^{\frac{n-1}{2}}$ as a free parameter which allows the following simple closed-form solution to equation 5 satisfying the initial conditions.

$$Y = -Q\left[\frac{X\cos^{n-2}\phi}{(n-2)} + \frac{Q\cos^{2n-2}\phi\left(\left(1-\frac{X\,n}{Q\cos^n\phi}\right)^{\frac{2n-2}{n}}-1\right)}{2(n-1)(n-2)}\right] + \frac{\tan\phi\,V_0\,V'|_0\,X}{g}. \tag{6}$$

Note the last expression becomes identical to the results presented in Weinacht et al. (*1*) when $\phi << 1$, thus making $\cos\phi \to 1$ and $Q \to 1$. Since the remainder of this report stems from manipulations of equation 6, it causes all following results given here to have similar identical behavior to Weinacht et al. (*1*) whenever the launch angle becomes small. This report will show equation 6 gives good solutions to the parameterized equation 5 for elevation angles $0 \le \phi \le 30°$ by using $Q = \cos^{1-n}\frac{6\phi}{7}$. This choice for Q was obtained using trial and error while comparing numerical solutions of equation 5 to those of equation 6, starting with $Q = 1$. The authors have judged the given value for Q is adequate for $0 \le \phi \le 30°$. The following presentation primarily focuses on $\phi = 30°$ since these cases were found to display the weakest agreement of all launch angles in the range $0 \le \phi \le 30°$. However, a few excursions with $\phi = 45°$ are discussed to indicate the limitations of $Q = \cos^{1-n}\frac{6\phi}{7}$ for $\phi > 30°$.

For completeness, the limiting cases for equation 6 are given in the following expressions:

$$Y - \frac{\tan\phi\, V_0\, V'|_0\, X}{g} \rightarrow \begin{cases} \dfrac{Q\left(Q + 2X - Q\,e^{\frac{2X}{Q}}\right)}{4\cos^2\phi}, n \rightarrow 0 \\ Q^2 \log\left(\dfrac{X^2}{Q^2\cos^2\phi} - \dfrac{2X}{Q\cos\phi} + 1\right)^{\frac{1}{2}} + \dfrac{X}{\cos\phi}, n \rightarrow 1 \\ \left.\begin{array}{l} \dfrac{QX}{4}\log\left(\dfrac{4X^2 - 4Q\cos^2\phi\, X + Q^2\cos^4\phi}{Q^2\cos^4\phi}\right) - \\ \dfrac{Q^2\cos^2\phi}{4}\log\left(1 - \dfrac{2X}{Q^2\cos^2\phi}\right) - \dfrac{QX}{2} \end{array}\right\}, n \rightarrow 2. \end{cases} \quad (7)$$

The choices of projectiles are the same as those used in Weinacht et al. (*1*) and the pertinent data are taken from table 1.

Table 1. Projectile characteristics.

Projectile Type	**Muzzle Velocity V_0 (m/s)**	**Muzzle Retardation $V'|_0$ ([m/s]/km**	$\frac{V'|_0}{V_0}$ **(1/km)**
M829A1	1580	68	0.043
M865PIP	1700	343	0.202
M830	1140	273	0.239
M830A1	1410	209	0.148

Comparative examples illustrating the validity of the parameterized solution equation 6 to the numerical solution of equation 5 are given in figure 1. The agreement between the two types of solutions is very strong except where the trajectory slope is steep for the M865PIP projectile.

The slope of the trajectories shown in figure 1 is given in figure 2, where it is evident that the analytic solutions agree with the numerical solutions. However, the particular case, M865PIP, has weaker agreement but this can be attributed to the much steeper slope and the fact that derivatives of an approximation usually don't agree as well as the given approximation.

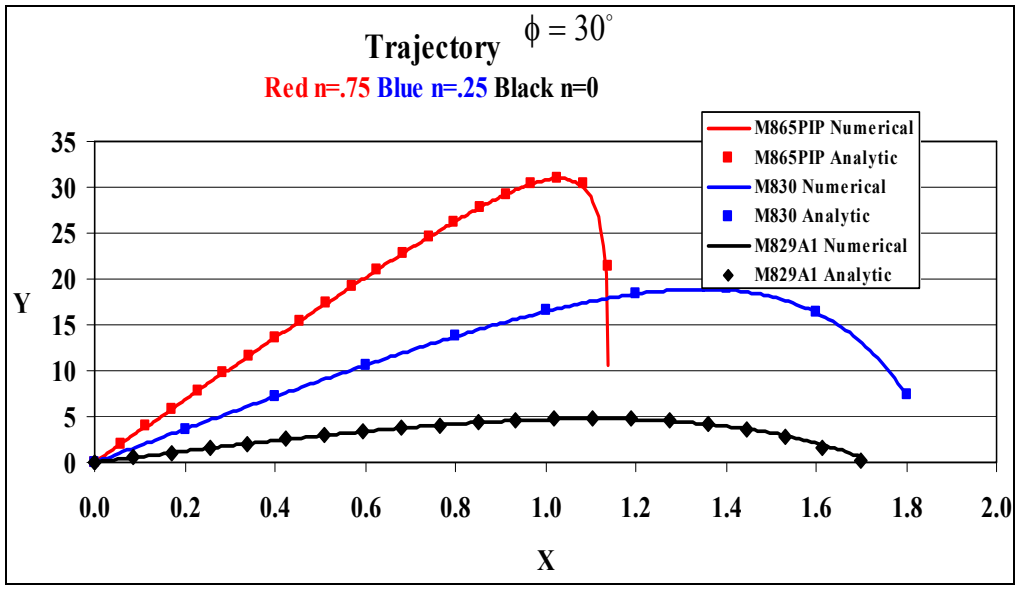

Figure 1. Comparison of analytic and numeric trajectories.

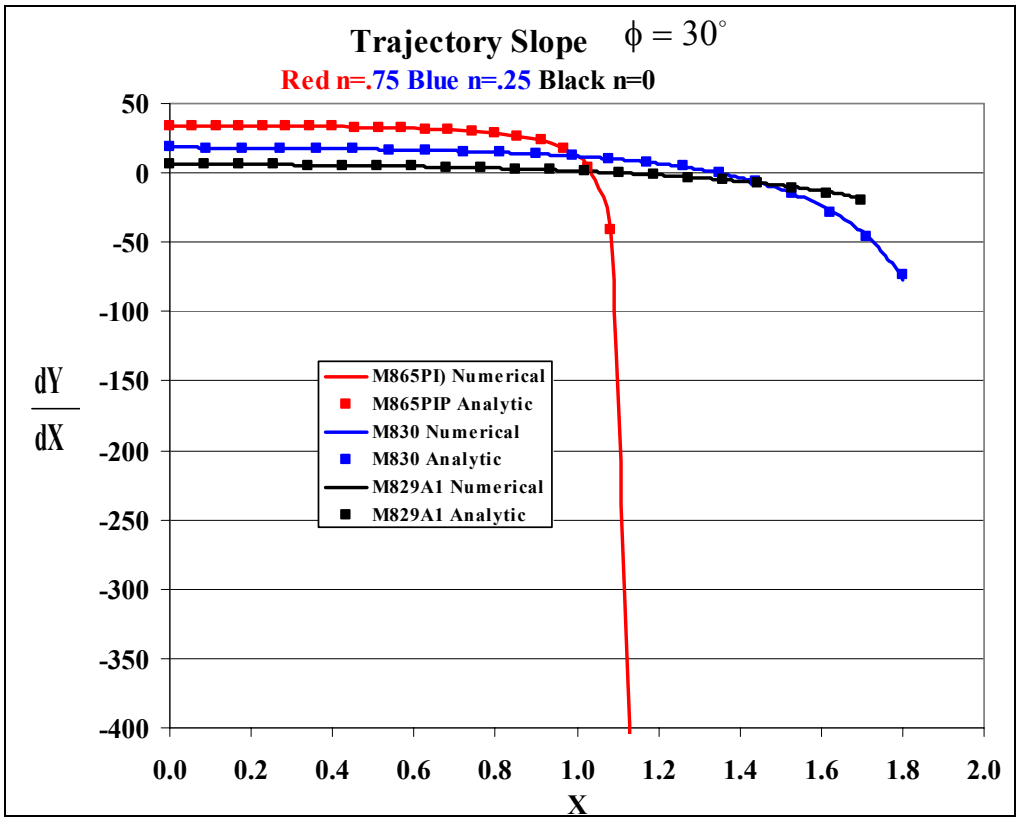

Figure 2. Comparison of analytic and numeric trajectory slopes.

Velocity components are readily obtained from equation 6 and limiting values from equation 7 produce the following expressions:

$$\dot{x} = V_0 \cos\phi \left(1 - \frac{n\,X}{Q \cos^n \phi}\right)^{\frac{1}{n}}$$

$$\rightarrow V_0 \cos\phi\, e^{\frac{-X}{Q}} \quad n \rightarrow 0$$

$$\dot{y} = \dot{x}\left[\frac{g\,Q \cos^{n-2}\phi}{V_0\, V'|_0\,(n-2)}\left(1 - \frac{n\,X}{Q\cos^n\phi}\right)^{\frac{n-2}{n}} + \tan\phi\right]$$

$$\rightarrow \dot{x}\left[\frac{g\,Q}{2\,V_0\,V'|_0 \cos^2\phi}\left(1 - e^{\frac{2X}{Q}}\right) + \tan\phi\right] \quad n \rightarrow 0$$

$$\rightarrow \dot{x}\left[\frac{g\,Q \log\left(1 - \frac{2\,X}{Q\cos^2\phi}\right)}{2\,V_0\,V'|_0} + \tan\phi\right] \quad n \rightarrow 2\,. \tag{8}$$

Figure 3 shows Mach number M profiles calculated from the last set of equations where comparisons are made to numerical solutions generated from equation 5.

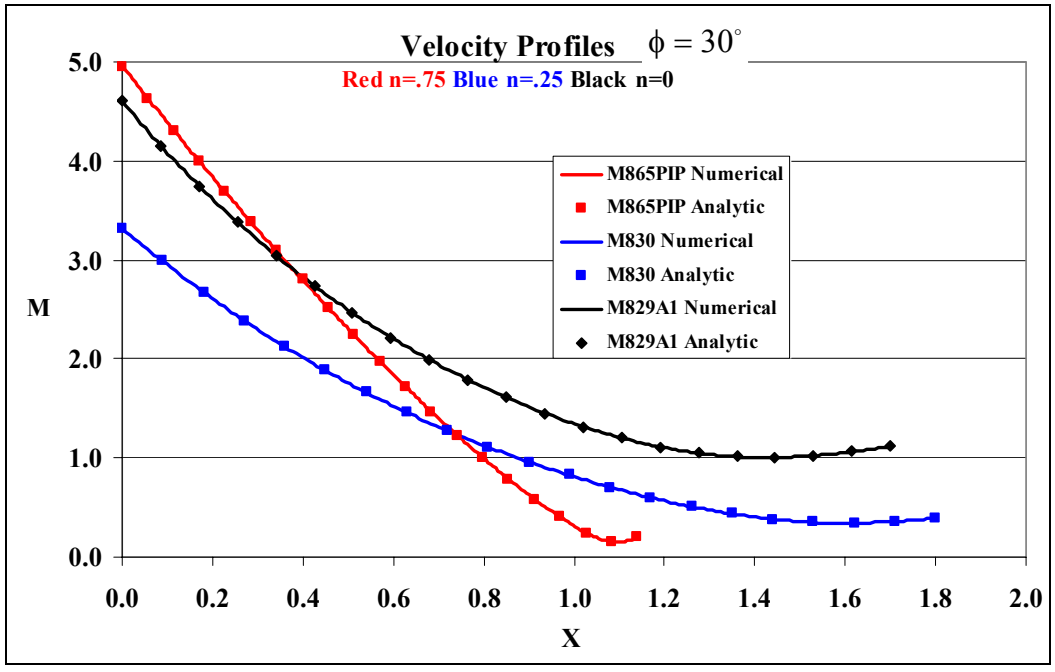

Figure 3. Comparison of numerical and analytic Mach number profiles.

The last set of plots also show that the weakest agreement of Y and $\frac{dY}{dX}$, figures 1 and 2, occurs when the Mach number M<1. Since the power-law drag formulation, equation 2, is usually considered for M>1, it suggests that the given results for $\phi \leq 30°$ are more applicable for ranges where M>1. Examples of the types of errors that occur when $\phi > 30°$ are shown in figure 4, where $\phi = 45°$.

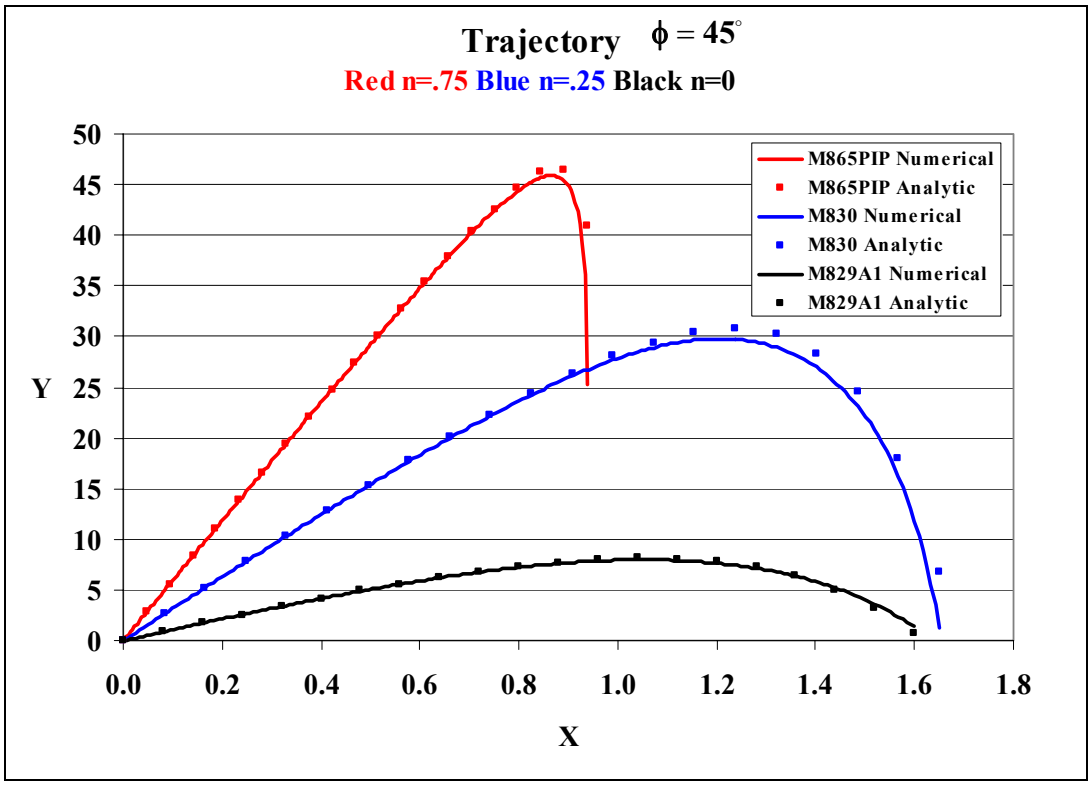

Figure 4. Comparison of analytic and numeric trajectories for φ = 45.

These results may be interpreted as an indication that $0 \leq \phi \leq 30°$ is an over-restriction for the ranges where M>1.

3. Gravity Drop

Analytical results of the previous work (*1*) regarding gravity drop were obtained by considering dimensional *y* terms that are dependent on *g*. Applying this last statement to the analysis given here simply means to set the term proportional to g^{-1} in equations 6 and 7 to zero to get scaled versions of gravity drop "Y_{g-drop}." Furthermore, expanding this expression in a Taylor series and converting the series to a rational function, thus increasing the range of validity, yields the following expression:

$$Y_{g-drop} \approx \frac{\cos^{n-2}\phi\, Q\, X^2 \left(2\left(3n+1\right)X - 15\cos\phi\right)}{3\left(\left(n+2\right)X\left(X - 4\,Q\cos^{n}\phi\right) + 10\,Q^2\cos^{2n}\phi\right)}. \tag{9}$$

Figure 5 has examples of gravity drop for the M865PIP projectile at various values of the drag-curve parameter *n*. Evidently, Y_{g-drop} is well approximated by equation 9.

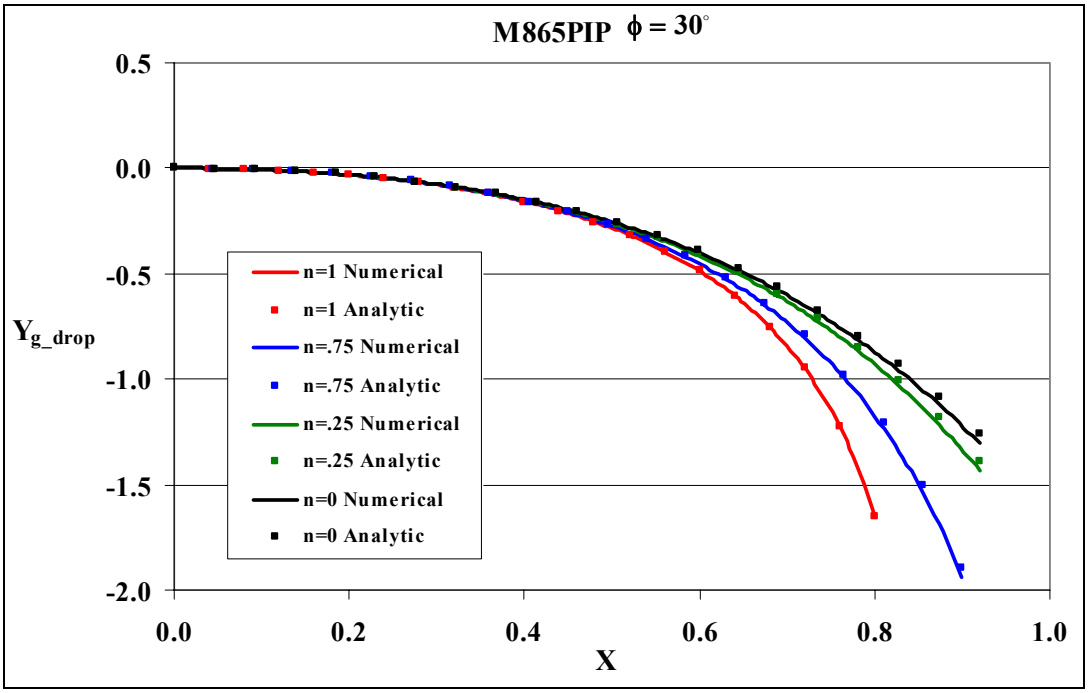

Figure 5. Comparison of numerical and analytic gravity drop for the M865PIP.

4. Gun Elevation and Target Position

Predicting the gun elevation angle ϕ to acquire a target at $Y = 0$, for a given range position X, is a useful flight parameter (*1*) that can be found from equation 6. Using the result for Y_{g-drop} given in equation 9 shows the elevation angle satisfies

$$\frac{V_0\, V'|_0 \tan\phi}{g} \approx \frac{-\cos^{n-2}\phi\, Q\, X\left(2\left(3n+1\right)X - 15\cos\phi\right)}{3\left(\left(n+2\right)X\left(X - 4\,Q\cos^{n}\phi\right) + 10\,Q^2\cos^{2}\phi\right)}. \tag{10}$$

Solving this expression for ϕ as large as 30° generally will require numerical techniques. But limiting analysis to small angles, $\phi << 1 \Rightarrow \cos\phi \to 1$ and $Q \to 1$, allows equation 10 to give direct solutions for small ϕ. These values are the same as those found in Weinacht et al. (*1*) and are repeated here for completeness in figure 6.

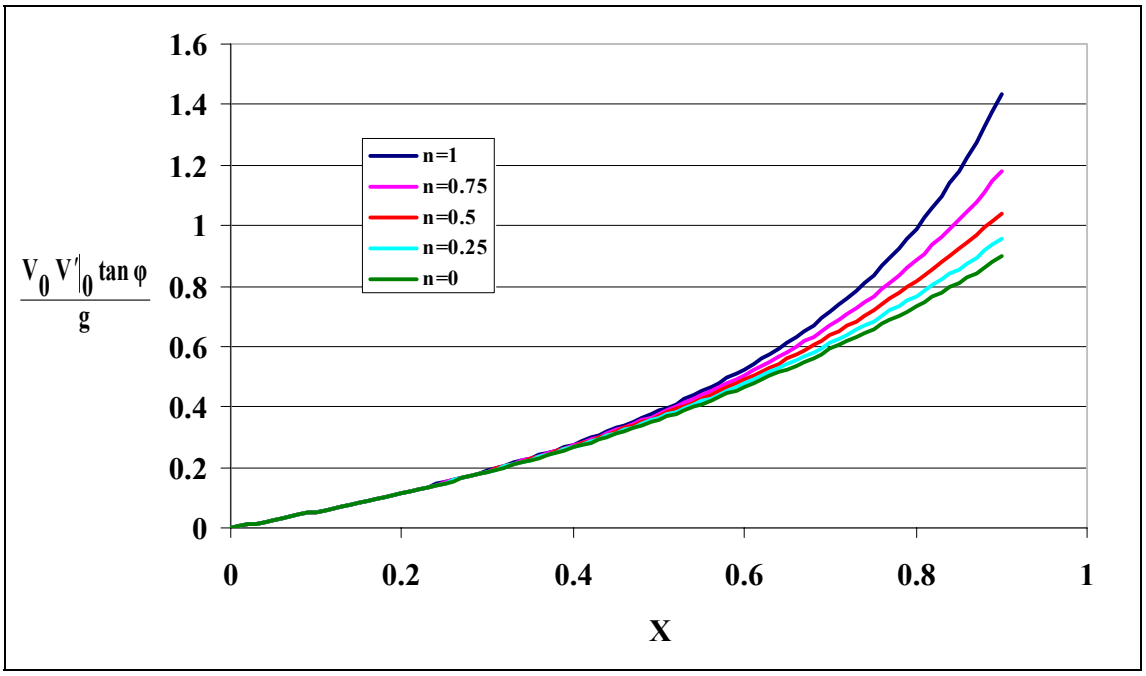

Figure 6. Scaled gun elevations as a function of scaled range.

5. Trajectory Rate of Change Due to Muzzle Velocity

The rate of vertical change of trajectory due to muzzle velocity V_0 can change significantly with range. An analytic expression for this comes directly from equation 6 and the dimensional rate of change scaled as $\frac{V_0 V'|_0}{g}\frac{dy}{dV_0} = V_0\frac{dY}{dV_0}$ is shown in the following expressions:

$$V_0\frac{dY}{dV_0} = \frac{Q^2\cos^{2n-2}\phi}{n(n-2)}\left[\left(1-n\frac{X}{Q\cos^n\phi}\right)^{\frac{2n-2}{n}} - \left(1-n\frac{X}{Q\cos^n\phi}\right)^{\frac{n-2}{n}} + n\frac{X}{Q\cos^n\phi}\right]$$

$$\rightarrow \frac{QX\left(1-e^{\frac{2X}{Q}}\right)}{2\cos^2\phi}\; n\rightarrow 0$$

$$\rightarrow \frac{QX}{2}\log\left(1-\frac{2X}{Q\cos^2\phi}\right)\; n\rightarrow 2. \qquad (11)$$

To validate equation 11, the derivative of equation 5 with respect to V_0 is numerically integrated. Results given in figure 7 compare the parameterized analytic solution to the nonparametric numerical solution.

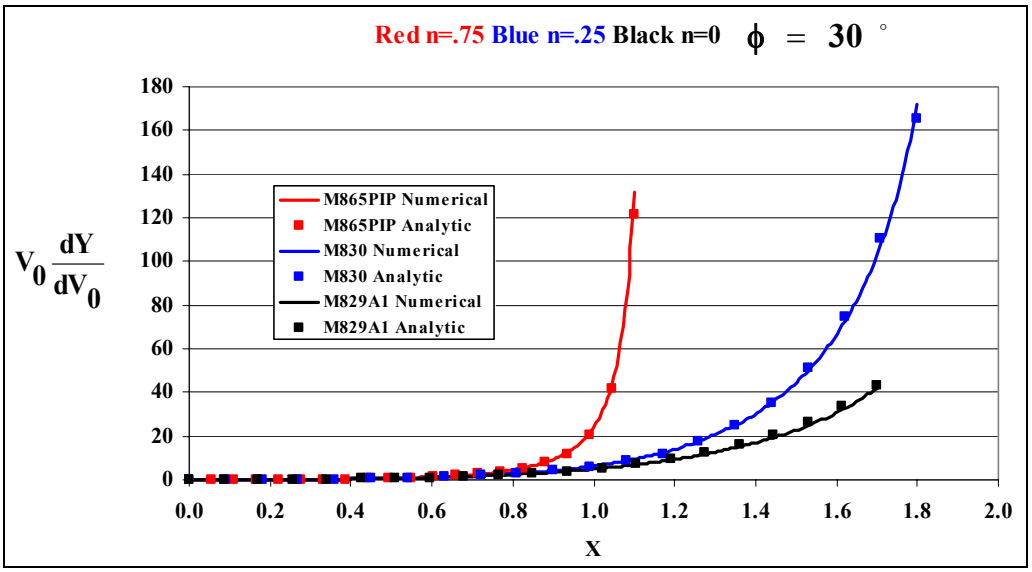

Figure 7. Comparison of scaled numerical and analytic dy/dV_0.

Figure 7 shows equation 11 is a good approximation to the rate of change of the trajectory caused by varying the muzzle velocity V_0.

6. Trajectory Rate of Change Due to Muzzle Retardation

The rate of vertical change in the trajectory as a function of the drag coefficient or muzzle retardation $V'|_0$ can also be an important influence on trajectory that depends on range. Again, equation 6 is used to find a scaled version of this rate of change.

$$V'|_0 \frac{dY}{dV'|_0} = \frac{Q^2 \cos^{2n-2}\phi}{n-2}\left[\frac{\left(1-\frac{nX}{Q\cos^n\phi}\right)^{\frac{2n-2}{n}}-1}{n-1}+\frac{X}{Q\cos^n\phi}\left(\left(1-\frac{nX}{Q\cos^n\phi}\right)^{\frac{n-2}{n}}+1\right)\right]$$

$$\rightarrow \frac{-Q}{2\cos^2\phi}\left((X-Q)e^{\frac{2X}{Q}}+X+Q\right) \; n\rightarrow 0$$

$$\rightarrow -2Q^2\log\left(1-\frac{X}{Q\cos\phi}\right)-\frac{QX\left(\frac{X}{Q\cos\phi}-2\right)}{\cos\phi\left(\frac{X}{Q\cos\phi}-1\right)}, n\rightarrow 1$$

$$\rightarrow QX-\frac{Q^2\cos^2\phi}{2}\left(\frac{X}{Q\cos^2\phi}-1\right)\log\left(1-\frac{2X}{Q\cos^2\phi}\right) \; n\rightarrow 2. \qquad (12)$$

Comparing these expressions to the numerical integration of the derivative of equation 5 with respect to $V'|_0$ is shown in figure 8. The case $n = 0.25$ shows the analytic solution degrades with increasing range. Once again, this is not too surprising since the derivative of a well-converged approximate function suffers with less convergence.

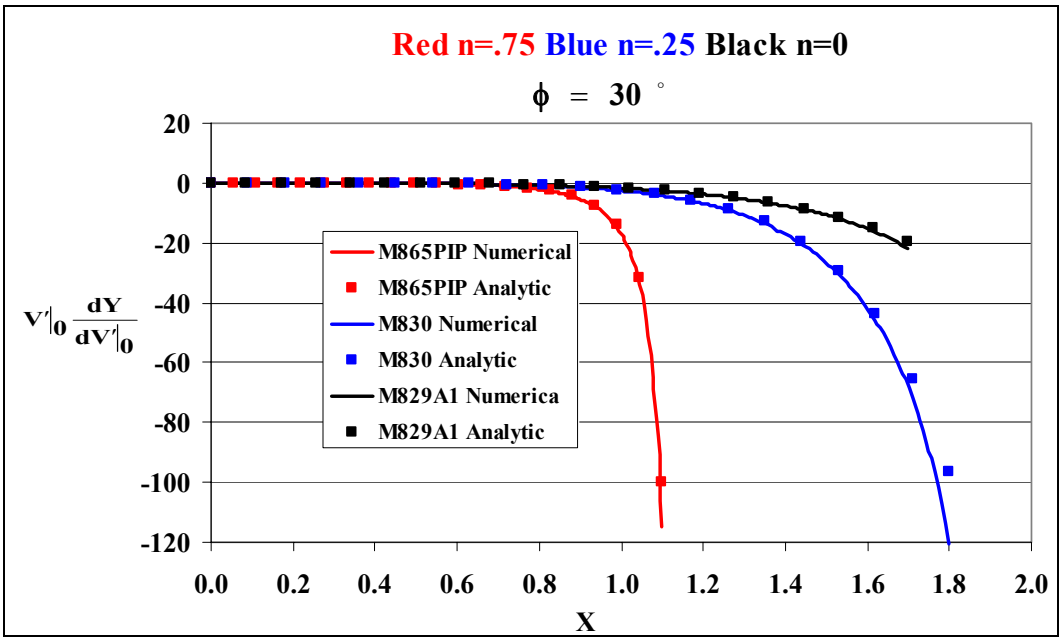

Figure 8. Comparison of scaled numerical and analytic $d\,y/d\,V'|_0$.

7. Time as the Independent Variable

The presentation given here has considered *x* as the independent variable but all of the previous results could be given in terms of the time *t* if desired. Integrating the first equation in equation 2 leads to an expression of *t* as a function of the scaled range *X* given by

$$
\begin{aligned}
t\,V'|_0 &= Q\cos^{n-1}\phi\,\frac{\left(1-\dfrac{nX}{Q\cos^n\phi}\right)^{\frac{n-1}{n}}}{n-1} \\
&\to \frac{Q\,e^{\frac{X}{Q}}}{\cos\phi}\,,\ n\to 0 \\
&\to -\frac{Q}{V'|_0}\log\left(V_0\,Q\cos\phi+1-\frac{X}{Q\cos\phi}\right),\ n\to 1.
\end{aligned}
\tag{13}
$$

Validation of equation 13 is displayed in figure 9, where it is evident that this expression supplies an accurate method to covert the scaled spatial independent variable X to the scaled temporal variable $\mathbf{t}\,\mathbf{V}'|_0$. Some error is introduced for the M865PIP projectile which can be attributed to the rapidly decreasing slope for X > 1 (see figure 2). This may not be a serious defect due to the relative small Mach number for X in this range.

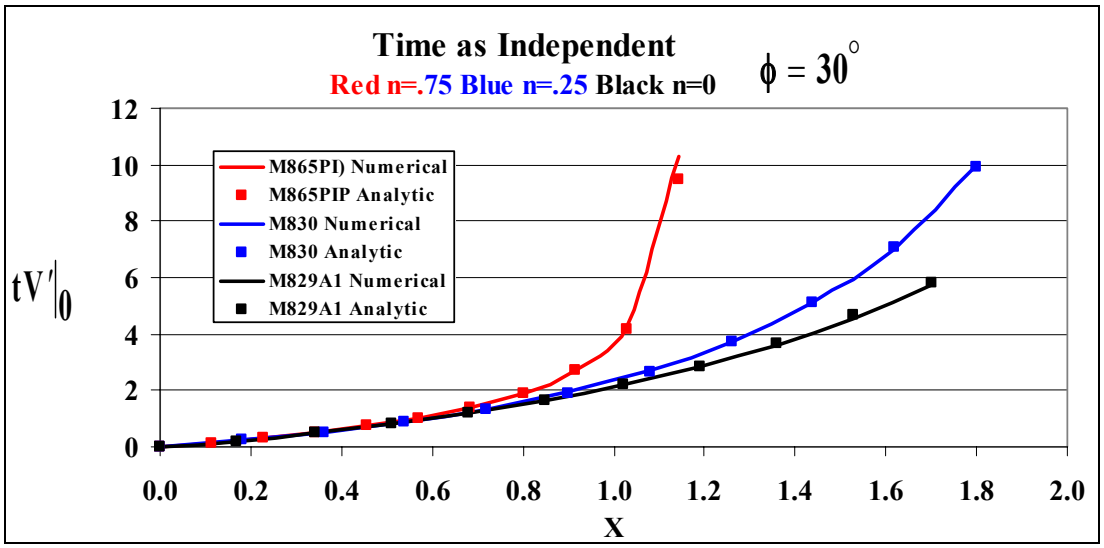

Figure 9. Comparison of scaled time as a function of scaled range.

8. Low Velocity Projectile

All of the investigations in this report have thus far focused on projectiles with high Mach number launch velocities. Therefore, suspicions may arise when applying this theory to projectiles with low launch velocities. To address this issue implies considering a sample of a relatively low launch velocity projectile. One such projectile is Scorpion, which has a typical launch velocity of V_0 = 76 m/s and a muzzle retardation of $V'|_0 = 104\,([\text{m/s}]/\text{km})$. Figures 10 and 11 have examples of subjecting Scorpion to the theory of this report using the usual value of n = 0 for subsonic launch velocities.

Evidently, the parametric results for low velocities agree as well as they do for high Mach number projectiles with launch angles $0 \le \phi \le 30°$. When $\phi = 45°$, the agreement has degraded but this agreement may still be strong enough to suggest that $\phi \le 30°$ is somewhat over-restrictive.

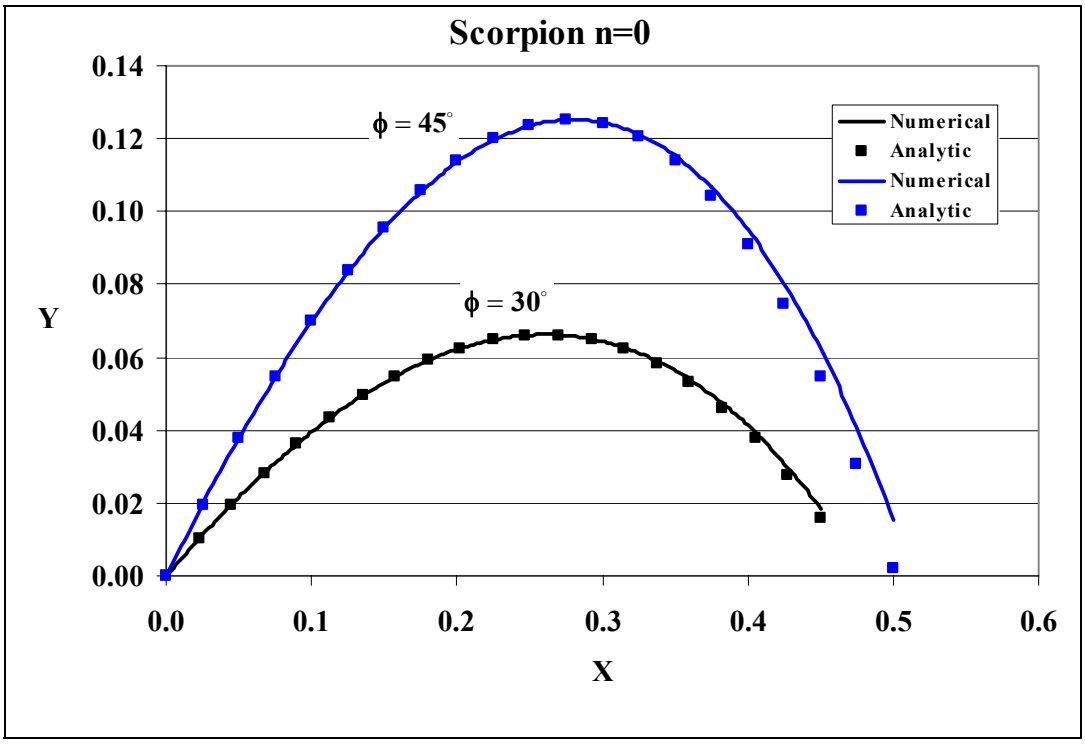

Figure 10. Comparison of trajectory calculations for Scorpion.

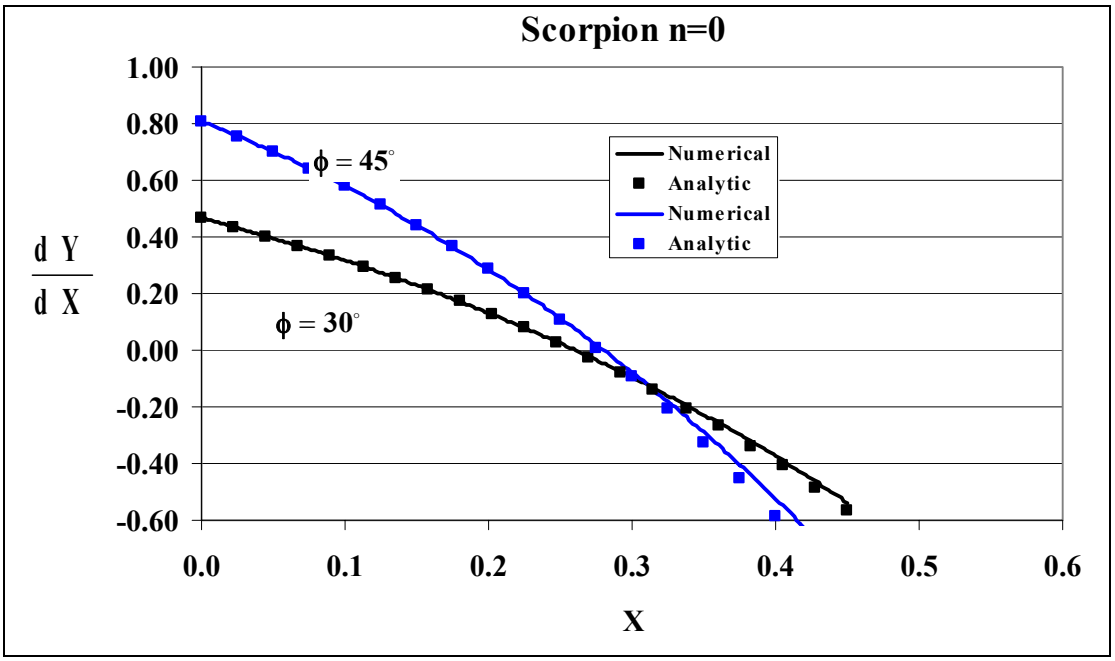

Figure 11. Comparison of trajectory slope calculations for Scorpion.

9. Summary

This report extends the investigation found in Weinacht et al. (*1*) which considered direct-fire, high-velocity projectiles subjected to power-law drag curves. The extension here continues to assume power-law drag curves but now the launch angle ϕ takes on values as large as $\phi = 30°$. In Weinacht et al. (*1*), gravity is treated as a small perturbation when projectile velocities are high. However, in this report, the equations of motion are written as a third-order nonlinear differential equation, DE, where range is the independent variable. A simple analytic solution to the DE is found by assuming a factor in this DE can be treated as a fixed parameter Q. A value for $Q = \cos^{1-n}\frac{6\phi}{7}$ is shown to produce valid solutions for launch angles $0 \le \phi \le 30°$ and, in the limit of $\phi \to 0$, yields solutions identical to those given in Weinacht et al. (*1*). Experience has shown the validity of the parameterized solutions increases as ϕ becomes smaller and, in fact, if $Q = 1$ for $0 \le \phi \le 20°$, produces accurate solutions. Examples where $\phi = 45°$ characterize the errors and trajectory degradation that occurs when the launch angle is greater than 30°, which may further indicate that $0 \le \phi \le 30°$ may be too restrictive. Replacing the spatial dependency to temporal dependency is easily accomplished by application of equation 13. Results given here can be used in engineering applications that are similar those discussed in Weinacht et al. (*1*), but now the launch angle ϕ can be as large as $\phi = 30°$.

10. References

1. Weinacht, P.; Cooper, G. R.; Newill, J. F. *Analytical Prediction of Trajectories for High-Velocity Direct-Fire Munitions;* ARL-TR-3567; U.S. Army Research Laboratory: Aberdeen Proving Ground, MD, August 2005.

2. McCoy, R. L. *Modern Exterior Ballistics*; Schiffer Military History: Atglen, PA, 1999.

3. McShane, E. J.; Kelley, J. L.; Reno, F. V. *Exterior Ballistics*; University of Denver Press: Denver, CO, 1953.

4. Pejsa, A. J. *Modern Practical Ballistics*; 2nd ed.; Kenwood Publishing: Minneapolis, MN, 1991.

5. Celmins, I. *Projectile Supersonic Drag Characteristics*; BRL-MR-3843; U.S. Army Ballistic Research Laboratory: Aberdeen Proving Ground, MD, July 1990.

List of Symbols, Abbreviations, and Acronyms

C_D	Drag coefficient
$C_D\|_{V_0}$	Launch drag coefficient
D	Reference diameter
g	Gravitational acceleration
m	Projectile mass
M	Mach number
n	Exponent of drag power law
S	Reference area $S = \pi D^2/4$
t	Time
V	Total velocity
V_0	Muzzle velocity
x	Dimension down-range distance
y	Dimension vertical distance
$V'\|_0$	Muzzle retardation
ϕ	Initial gun elevation angle
ρ	Atmospheric density

NO. OF
COPIES ORGANIZATION

1 (PDF ONLY) DEFENSE TECHNICAL INFORMATION CTR
DTIC OCA
8725 JOHN J KINGMAN RD
STE 0944
FORT BELVOIR VA 22060-6218

1 US ARMY RSRCH DEV & ENGRG CMD
SYSTEMS OF SYSTEMS INTEGRATION
AMSRD SS T
6000 6TH ST STE 100
FORT BELVOIR VA 22060-5608

1 DIRECTOR
US ARMY RESEARCH LAB
IMNE ALC IMS
2800 POWDER MILL RD
ADELPHI MD 20783-1197

3 DIRECTOR
US ARMY RESEARCH LAB
AMSRD ARL CI OK TL
2800 POWDER MILL RD
ADELPHI MD 20783-1197

ABERDEEN PROVING GROUND

1 DIR USARL
AMSRD ARL CI OK TP (BLDG 4600)

NO. OF COPIES ORGANIZATION

1 PROD MGR
SML AND MEDM CAL AMMO
SFAE AMO MAS SMC
LTC M BULTER
BLDG 354
PICATINNY ARSENAL NJ
07806-5000

1 PROJ MNGR MNVR AMMO SYS
SFAE AMO MAS SMC
R KOWALSKI
BLDG 354
PICATINNY ARSENAL NJ
07806-5000

1 ATK
R DOHRN
MN07 LW54
4700 NATHAN LANE N
PLYMOUTH MN 55442

1 ATK
C AAKHUS
MN07 LW54
4700 NATHAN LANE N
PLYMOUTH MN 55442

1 ATK
M JANTSCHER
N07 LW54
4700 NATHAN LANE N
PLYMOUTH MN 55442

1 ATK LAKE CITY
K ENLOW
PO BOX 1000
INDEPENDENCE MO 64051-1000

5 ATK LAKE CITY
SML CAL AMMO
LAKE CITY ARMY AMMO PLANT
D MANSFIELD
PO BOX 1000
INDEPENDENCE, MO 64051-1000

1 ATK LAKE CITY
MO10 003
LAKE CITY ARMY AMMO PLANT
J WESTBROOK
PO BOX 1000
INDEPENDENCE MO 64051-1000

NO. OF COPIES ORGANIZATION

1 ALLIANT TECHSYSTEMS INC
D KAMDAR
MN07 LW54
4700 NATHAN LANE N
PLYMOUTH MN 55442-2512

1 ATK ORDNANCE SYS
B BECKER
MN07 MW44
4700 NATHAN LANE N
PLYMOUTH MN 55442-2512

1 US ARMY TACOM ARDEC
CCAC AMSTA AR CCL C
G FLEMING
BLDG 65N
PICATINNY ARSENAL NJ
07806-5000

1 US ARMY TACOM ARDEC
CCAC AMSTA AR CCL B
J MIDDLETON
BLDG 65N
PICATINNY ARSENAL NJ
07806-5000

1 US ARMY TACOM ARDEC
ASIC PRGRM INTGRTN OFC
J RESCH
BLDG 1
PICATINNY ARSENAL NJ
07801

1 US ARMY TACOM ARDEC
M MINISI
BLDG 65
PICATINNY ARSENAL NJ
07806-5000

1 US ARMY TACOM ARDEC
S SPICKERT FULTON
BLDG 65N
PICATINNY ARSENAL NJ
07806-5000

NO. OF
COPIES ORGANIZATION

1 US ARMY TACOM ARDEC
M NICOLICH
BLDG 65S
PICATINNY ARSENAL NJ
07806-5000

1 US ARMY TACOM ARDEC
AMSTA AR CCH A
S MUSALLI
BLDG 65S
PICATINNY ARSENAL NJ
07806-5000

1 US ARMY TACOM ARDEC
AMSRD AAR AEM I
R MAZESKI
BLDG 65N
PICATINNY ARSENAL NJ
07806-5000

1 US ARMY TACOM ARDEC
A FARINA
BLDG 95
PICATINNY ARSENAL NJ
07806-5000

1 US ARMY TACOM ARDEC
CCAC
AMSTA AR CCL B
D CONWAY
BLDG 65N
PICATINNY ARSENAL NJ
07806-5000

1 US ARMY TACOM ARDEC
AMSTA AR FSF T
H HUDGINS
BLDG 382
PICATINNY ARSENAL NJ
07806-5000

1 US ARMY TACOM ARDEC
CCAC
AMSTA AR CCL D
F HANZL
BLDG 354
PICATINNY ARSENAL NJ
07806-5000

NO. OF
COPIES ORGANIZATION

1 US ARMY TACOM ARDEC
P RIGGS
BLDG 65N
PICATINNY ARSENAL NJ
07806-5000

1 OPM MAS
SFAE AMO MAS MC
G DEROSA
BLDG 354
PICATINNY ARSENAL NJ
07806 5000

2 COMMANDER
US ARMY TACOM ARDEC
AMSTR AR FSF X
W TOLEDO
BLDG 95 S
PICATINNY ARSENAL NJ
07806-5000

ABERDEEN PROVING GROUND

20 DIR USARL
AMSRD ARL WM
J SMITH
AMSRD AR WM B
M ZOLTOSKI (2 CPS)
AMSRD AR WM BA
D LYON
AMSRD ARL WM BD
P CONROY
B FORCH
AMSRD ARL WM BC
G COOPER (3 CPS)
B GUIDOS
J NEWILL
P PLOSTINS
S SILTON
P WEINACHT
AMSRD ARL WM BD
M NUSCA
AMSRD ARL WM BF
W OBERLE
R PEARSON
AMSRD ARL WM TA
M BURKINS
AMSRD ARL WM TC
L MAGNESS
B PETERSON

INTENTIONALLY LEFT BLANK.